The Journal of Toxicological Sciences (J. Toxicol. Sci.)
Vol.48, No.3, 121-137, 2023

Original Article

Amelioration of lipopolysaccharides-induced impairment of fear memory acquisition by alpha-glycosyl isoquercitrin through suppression of neuroinflammation in rats

Qian Tang[1,2], Kazumi Takashima[1,2], Wen Zeng[1], Hiromu Okano[1,2], Xinyu Zou[1,2], Yasunori Takahashi[1,2], Ryota Ojiro[1,2], Shunsuke Ozawa[1,2], Mihoko Koyanagi[3], Robert R. Maronpot[4], Toshinori Yoshida[1,2] and Makoto Shibutani[1,2,5]

[1]Laboratory of Veterinary Pathology, Tokyo University of Agriculture and Technology, 3-5-8 Saiwai-cho, Fuchu-shi, Tokyo 183-8509, Japan
[2]Cooperative Division of Veterinary Sciences, Graduate School of Agriculture, Tokyo University of Agriculture and Technology, 3-5-8 Saiwai-cho, Fuchu-shi, Tokyo 183-8509, Japan
[3]Global Scientific and Regulatory Affairs, San-Ei Gen F.F.I., Inc., 1-1-11 Sanwa-cho, Toyonaka, Osaka 561-8588, Japan
[4]Maronpot Consulting, LLC, 1612 Medfield Road, Raleigh, North Carolina 27607, USA
[5]Institute of Global Innovation Research, Tokyo University of Agriculture and Technology, 3-5-8 Saiwai-cho, Fuchu-shi, Tokyo 183-8509, Japan

[Contributed by Makoto Shibutani]

(Received November 21, 2022; Accepted November 21, 2022)

ABSTRACT — This study investigated the role of neuroinflammation in a lipopolysaccharides (LPS)-induced cognitive dysfunction model in rats using an antioxidant, α-glycosyl isoquercitrin (AGIQ). Six-week-old rats were dietary treated with 0.5% (w/w) AGIQ for 38 days, and LPS at 1 mg/kg body weight was administered intraperitoneally once daily on Days 8 and 10. On Day 11, LPS alone increased or tended to increase interleukin-1β and tumor necrosis factor-α in the hippocampus and cerebral cortex. Immunohistochemically, LPS alone increased the number of Iba1$^+$ and CD68$^+$ microglia, and GFAP$^+$ astrocytes in the hilus of the hippocampal dentate gyrus (DG). AGIQ treatment decreased or tended to decrease brain proinflammatory cytokine levels and the number of CD68$^+$ microglia in the DG hilus. In the contextual fear conditioning test during Day 34 and Day 38, LPS alone impaired fear memory acquisition, and AGIQ tended to recover this impairment. On Day 38, LPS alone decreased the number of DCX$^+$ cells in the neurogenic niche, and AGIQ increased the numbers of PCNA$^+$ cells in the subgranular zone and CALB2$^+$ hilar interneurons. Additionally, LPS alone decreased or tended to decrease the number of synaptic plasticity-related FOS$^+$ and COX2$^+$ granule cells and AGIQ recovered them. The results suggest that LPS administration induced acute neuroinflammation and subsequent impairment of fear memory acquisition caused by suppressed synaptic plasticity of newborn granule cells following disruptive neurogenesis. In contrast, AGIQ exhibited anti-inflammatory effects and ameliorated LPS-induced adverse effects. These results suggest that neuroinflammation is a key factor in the development of LPS-induced impairment of fear memory acquisition.

Key words: Alpha-glycosyl isoquercitrin (AGIQ), Fear memory acquisition, Hippocampal neurogenesis, Lipopolysaccharides (LPS), Neuroinflammation, Rat

INTRODUCTION

Depression is a common psychiatric disorder characterized by an abnormal depressed mood, lack of pleasure, and appetite or weight disturbance (Haroz *et al*., 2017). The etiology of depression is complex, and in recent

Correspondence: Makoto Shibutani (E-mail: mshibuta@cc.tuat.ac.jp)

years neuroinflammation and disruption of hippocampal neurogenesis have been identified as key risk factors for a number of mental disorders, including depression (Dantzer *et al*., 2008; Hanson *et al*., 2011). Therefore, prevention of neuroinflammation and disruptive neurogenesis is of clinical importance for the treatment of depression. Studies have shown increased inflammatory cytokines in the peripheral blood and brain of depressed patients (Beurel *et al*., 2020). It has been demonstrated that peripheral inflammation can disrupt the blood-brain barrier by various pathways, resulting in a variety of cognitive and emotional dysfunctions (Huang *et al*., 2021). Lipopolysaccharides (LPS), a component of the cell wall of Gram-negative bacteria, activates the immune system through specific binding to Toll-like receptor 4. Studies have shown that systemic administration of LPS leads to oxidative stress in the hippocampus and prefrontal cortex, inducing depression-like symptoms such as increased anxiety and cognitive impairment in experimental animals (Taniguti *et al*., 2019). Microglia and astrocytes of the central nervous system are the mainstay of Toll-like receptor 4 expression, and in the presence of neuroinflammation from various sources, glial cells are involved in the regulation of neuroinflammatory responses and oxidative stress by activating downstream signaling cascades through the conversion of pro- and anti-inflammatory phenotypes (Gárate *et al*., 2011; Liu *et al*., 2020).

Chronic inflammation induces the release of neurotoxic substances, which may affect neurogenesis and plasticity (Song and Wang, 2011). The hippocampal dentate gyrus (DG) is the primary brain substructure of new neuron production during adulthood, where neuronal circuits are regulated by a variety of environmental or intrinsic factors that influence adult neurogenesis (Boldrini *et al*., 2018; Deroche-Gamonet *et al*., 2019). Type-1 neural stem cells (NSCs) located in the subgranular zone (SGZ) of the DG perform self-renewal while providing a source of output to neural progenitor cells (NPCs), which sequentially proliferate to type-2a, type-2b, and type-3 NPCs (Hodge *et al*., 2008). Type-3 NPCs undergo mitosis to become immature granule cells, eventually forming mature granule cells integrated into the granule cell layer (GCL) of the hippocampus (Kempermann *et al*., 2015). Multiple synaptic connections and signaling in the DG influence neurogenesis. The proliferation and differentiation of NSCs and NPCs in the DG are innervated by subpopulations of γ-aminobutyric acid (GABA)-ergic interneurons to maintain an appropriate granule cell population (Sibbe and Kulik, 2017). In addition to GABAergic inputs, neurons in the DG also receive glutamatergic, cholinergic, and dopaminergic neurotransmitter signals from outside the SGZ (Berg *et al*., 2013). Furthermore, synaptic plasticity of newly produced granule cells could be regulated through the modulation of adult neurogenesis (Moreno-Jiménez *et al*., 2021).

Alpha-glucosyl isoquercitrin (AGIQ) is a polyphenolic flavonol glycoside obtained from the enzymatic glycosylation of rutin, which is widely found in plants such as buckwheat, brassica and citrus fruits and is frequently ingested in our daily life (Akiyama *et al*., 2000). AGIQ, which consists of isoquercitrin and its α-glucosylated derivatives, is a mixture of quercetin glycosides with better bioavailability than the usual quercetin (Akiyama *et al*., 2000). AGIQ has been reported to have antioxidant (Kangawa *et al*., 2017), anti- allergic (Makino *et al*., 2013), anti-hypertensive (Gasparotto Junior *et al*., 2011), and tumor-inhibiting (Fujii *et al*., 2013) properties. Our previous study demonstrated that AGIQ-exposed offspring showed enhanced fear extinction learning in a contextual fear conditioning test and an increase in the number of granule cells immunoreactive for Fos proto-oncogene, AP-1 transcription factor subunit (FOS), a synaptic plasticity-related immediate-early gene (IEG) product, in the hippocampal DG, suggesting that exposure to AGIQ leads to increased synaptic plasticity (Okada *et al*., 2019). Furthermore, continuous AGIQ exposure after weaning ameliorated the suppressed hippocampal neurogenesis induced by developmental hypothyroidism through modulation of the antioxidant system and GABAergic interneuron subpopulations (Tanaka *et al*., 2019).

The present study investigated the role of neuroinflammation for development of cognitive dysfunction in a rat model of LPS-induced depression. For this purpose, we examined the effect of AGIQ as an antioxidant on behavioral abnormalities, neuroinflammation, oxidative stress and aberrations in hippocampal neurogenesis in adult rats by performing behavioral tests, biochemistry, immunohistochemistry and gene expression analysis.

MATERIALS AND METHODS

Chemicals and animals

Lipopolysaccharides (LPS) from *Escherichia coli* O55:B5 (EC No. 297-473-0, purity: 97%) were purchased from Sigma-Aldrich Co. LLC. (St. Louis, MO, USA). Alpha-glycosyl isoquercitrin (AGIQ, purity: > 97%) was provided by San-Ei Gen F.F.I. Inc. (Osaka, Japan). Five-week-old male Slc:SD rats (N = 92) acquired from Japan SLC, Inc. (Hamamatsu, Japan) were maintained in an air-conditioned animal room (temperature, 23 ± 2°C; relative humidity, 55 ± 15%) with a 12 hr light/12 hr dark cycle. Animals were reared with two or three animals per cage,

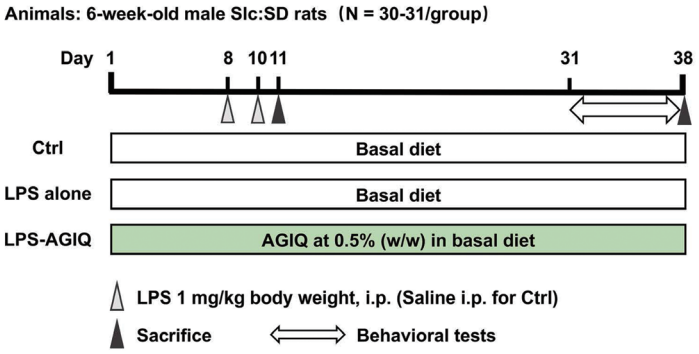

Fig. 1. Experimental design of exposure to lipopolysaccharides (LPS) at Day 8 and Day 10 of the experiment, accompanied with exposure to α-glycosyl isoquercitrin (AGIQ) from Day 1 to Day 38. On Day 8 and Day 10 at 48-hr intervals, male rats were intraperitoneally administered LPS at 1 mg/kg body weight/day except for those in the controls (Ctrl), which received vehicle saline solution. At Day 11, necropsy and tissue sampling were performed on 14 to 15 animals per group. The remaining animals were fed a diet with or without AGIQ until Day 38. Behavioral tests were performed using 10 animals per group during the period from Day 31 to Day 38 (i.e., open field test on Day 31 and Day 32 and contextual fear conditioning test on Day 34 to Day 38). At Day 38, necropsy and tissue sampling were performed on 16 animals per group. Animals subjected to behavioral tests were necropsied 90 min after the behavioral test was completed.

and allowed free access to a powdered basal diet (CRF-1; Oriental Yeast Co. Ltd., Tokyo, Japan) until the start of AGIQ exposure and tap water provided ad libitum throughout the experimental period.

Experimental design

A schematic of the experimental design is shown in Fig. 1. After six days of acclimation, animals were randomly assigned to three groups of 30 to 31 animals per group: controls, LPS-alone group, and LPS-AGIQ group. Animals in the LPS-AGIQ group were administered 0.5% (w/w) AGIQ in the powdered basal diet from the first day of the experiment (Day 1) to Day 38. AGIQ at 0.5% in the diet has been shown to promote fear extinction learning by continuous exposure from gestational day 6 to postnatal day 77 in rats (Okada *et al*., 2019; Masubuchi *et al*., 2020). On Day 8 and Day 10, animals were given two intraperitoneal injections of 1 mg/kg body weight/day of LPS at 48-hr intervals except for animals in the controls receiving vehicle saline solution. The dose of LPS was determined according to the dose that has been reported to cause depression-like behaviors (Salmani *et al*., 2018; Zhang *et al*., 2019). Body weight, food intake, and water consumption were measured daily on Days 8 to 11 and twice a week during the rest of the study period.

On Day 11, the next day of the second LPS administration, 14 to 15 animals per group were euthanized to assess LPS-induced neuroinflammation and oxidative stress in the immediate stage after LPS injection. For immunohistochemical analysis, 8 to 9 animals per group were perfusion-fixed with ice-cold 4% (w/v) paraformaldehyde (PFA) in 0.1 M phosphate buffer (pH 7.4) at a flow rate of 20 mL/min through the left cardiac ventricle after deep anesthesia with CO_2/O_2. Remaining 6 animals per group were perfused with ice-cold saline [0.9% (w/v) NaCl] at a flow rate of 20 mL/min through the left cardiac ventricle, and the brains were removed after deep anesthesia with CO_2/O_2. The right and left cerebral hemispheres were isolated on ice, and the left cerebral hemisphere was fixed with methacarn solution according to the whole brain fixation method for mRNA expression analysis (Akane *et al*., 2013). Hippocampal and prefrontal cortex tissues were isolated from the right cerebral hemisphere, immediately frozen in liquid nitrogen and stored at –80°C for measurement of proinflammatory cytokine and oxidative stress levels.

In order to assess LPS-induced behavioral abnormalities at the late stage after LPS administration, behavioral tests were performed during the last one week of the AGIQ treatment period with 10 animals per group, including the open field test and contextual fear conditioning test. On Day 38, 16 animals per group were euthanized to assess the adverse effects of LPS on hippocampal neurogenesis and synaptic plasticity at the late stage after LPS administration. For immunohistochemistry, the animals subjected to behavioral tests (10 animals per group) were subjected to perfusion fixation through the left cardiac ventricle with ice-cold 4% (w/v) PFA buffer solution at a flow rate of 25 mL/min under CO_2/O_2-induced anesthesia 90 min after the 5th trial of the contextual fear con-

ditioning test. For mRNA expression analysis, the other 6 animals in each group, which were not subjected to behavioral testing were euthanized by exsanguination from the abdominal aorta under CO_2/O_2 anesthesia, and brains were fixed with methacarn solution according to the whole brain fixation method after weighing.

All animals were checked each day to assess general condition based on abnormal gait and behaviors. All procedures in the present study were conducted in accordance with the National Institutes of Health guide for the care and use of laboratory animals (NIH Publications No. 8023, revised 1978) and according to the protocol approved by the Animal Care and Use Committee of the Tokyo University of Agriculture and Technology (Approved No.: R03-147, R03-187). All efforts were made to minimize animal suffering.

Behavioral tests

Open field test and contextual fear conditioning test were performed. Before performing each test, the animals were acclimatized to the behavioral test room for 1 hr to 2 hr. The apparatus was cleaned with 70% ethanol solution before and after each test. After the end of each behavioral test, the animals were promptly returned to their original cages and transferred to the animal room. All experiments were performed between 11:00 and 15:00. The order of animal selection for testing among groups was counterbalanced in terms of test time to avoid any bias in test times of each group.

Open field test

The open field test was performed on Day 31 and Day 32 to assess locomotor activity and anxiety-like behaviors. The arena consisted of a square stainless-steel tray and walls surrounding the tray (Supplementary Fig. 1A; 900 × 900 × 500 mm; O'Hara & Co., Ltd. Tokyo, Japan). Both tray and wall had a matte black polyvinyl plastic surface. The floor illuminance in the center of the arena was set at 10 lux. The test animal was placed at the corner of the arena with the head facing the wall and allowed to explore the arena freely for 10 min. The movement of animals was tracked using a CCD camera (WAT-902B; Watec Co., Ltd., Tsuruoka, Japan) mounted above the arena and evaluated by an automatic computer tracking system (TimeOFCR1 software; O'Hara & Co., Ltd.). In the tracking system, the testing arena was equally divided into 25 squares, and the 9 squares located in the central area were defined as the center region (Supplementary Fig. 1A). The total moving distance and percentage of time spent in the center region to the total exploration time (center region rate) were used as indicators of locomotor activity and anxiety behavior, respectively.

Contextual fear conditioning test

The contextual fear conditioning test was performed from Day 34 to Day 38 using animals subjected to the open field test to assess contextual and extinction learning. The animals were subjected to 5 trials at 24-hr intervals over 5 consecutive days: one fear conditioning trial with electronic footshock, one fear acquisition trial and three fear extinction trials without footshock (Supplementary Fig. 1B). All trials were carried out in a rodent observation cage (370 × 300 × 250 mm) constructed of Plexiglas that was placed in a sound-attenuating chamber (CL-4211; O'Hara & Co., Ltd.). The floor of the test chamber comprised of 21 steel rods through which a scrambled shock from a shock generator (SGA-2020; O'Hara & Co., Ltd.) was delivered. The chamber was kept at the background white noise at 50 dB, and at 200 lux luminance.

Contextual fear conditioning (1st trial): Animals were transferred to the observation cage and after 88, 148, and 238 sec, 2 sec of footshocks each time were delivered (0.3 mA intensity, a total of 3 footshocks). Sixty sec after the last footshock, the animals were transferred to the home cage from the observation cage. Thus, one trial took 5 min.

Fear acquisition (2nd trial): Twenty-four-hr after the conditioning, each animal was placed back into the original observation cage for 5 min, but during which no footshock was delivered.

Fear extinction (3rd, 4th, and 5th trials): Following 48, 72, and 96-hr of the conditioning, each animal was placed back into the original observation cage, for 5 min, but during which no footshock was delivered.

The movement of animals was video recorded by a CCD camera (WAT-902B; O'Hara & Co., Ltd.) mounted above the observation cage, and analyzed using an automatic video-tracking system (TimeFZ2 software; O'Hara & Co., Ltd.). The freezing rate was calculated as the percent of time the animal spent in freezing behavior for ≥ 5 sec during each of the trial time of 5 min. The freezing rate of the 2nd trial was used as an index of fear memory acquisition. The ratio of the freezing rate of each of the 3rd, 4th, and 5th trials to the 2nd trial (relative freezing rate) was also calculated and used as an index of fear extinction learning.

Quantitative analysis of proinflammatory cytokines and oxidative stress in the brain

The hippocampus and cerebral cortex were homogenized in RIPA Lysis Buffer (Santa Cruz Biotechnology, Dallas, TX, USA) and protein concentration of the homogenates was measured using Pierce™ BCA Protein Assay

Kit (Thermo Fisher Scientific Inc., Waltham, MA, USA), according to the manufacturer's instructions, to normalize concentration of proinflammatory cytokine and malondialdehyde (MDA) levels.

The levels of proinflammatory cytokines, including interleukin (IL)-1β, IL-6, and tumor necrosis factor (TNF)-α, in the hippocampus and cerebral cortex on Day 11 were measured using Quantikine ELISA (Rat IL-1β, IL-6, and TNF-α; R&D SYSTEMS, Minneapolis, MN, USA), according to the manufacturer's instructions. Each cytokine level was expressed as pg/mg protein.

As an index of oxidative stress, the amount of the MDA as lipid peroxidation end products in the hippocampus and cerebral cortex on Day 11 was measured using TBARS assay kit (Cayman Chemicals, Ann Arbor, MI, USA), according to the manufacturer's instructions. Briefly, the amount of MDA was measured spectrophotometrically at 532 nm by thiobarbituric acid reactive substance method. MDA level was expressed as nmol/mg protein.

Immunohistochemistry and apoptosis assay

The brains at Day 11 and Day 38 perfusion-fixed with 4% PFA buffer were used to prepare brain sections. Three mm-thick coronal slices were prepared using a brain matrix at –2.2 mm from the bregma and further fixed in 4% PFA buffer solution overnight at 4°C, processed for paraffin embedding, and then subjected to sectioning at 3 μm.

Brain sections of 8 and 10 animals per group at Day 11 and Day 38, respectively, were subjected to immunohistochemistry using primary antibodies shown in Supplementary Table 1: glial fibrillary acidic protein (GFAP), which is expressed in type-1 NSCs in the SGZ and astrocytes (Hodge *et al*., 2008; Sibbe and Kulik, 2017), SRY-box transcription factor 2 (SOX2), expressed in type-1 NSCs, type-2a NPCs, and type-2b NPCs in the SGZ (Hodge *et al*., 2008; Sibbe and Kulik, 2017), T-box brain protein 2 (TBR2), expressed in type-2b progenitor cells in the SGZ (Hodge *et al*., 2008; Sibbe and Kulik, 2017), doublecortin (DCX), which is expressed in type-2b and type-3 NPCs, and immature granule cells (Sibbe and Kulik, 2017), tubulin, beta 3 class III (TUBB3, also known as Tuj-1), expressed in postmitotic immature granule cells (von Bohlen Und Halbach, 2007), and neuronal nuclei (NeuN), which is expressed in postmitotic immature and mature granule cells in the SGZ and GCL (Sibbe and Kulik, 2017); parvalbumin (PVALB), reelin (RELN), calbindin-D-29K (CALB2), glutamic acid decarboxylase 67 (GAD67), and somatostatin (SST), which are expressed in GABAergic interneuron subpopulations (Freund and Buzsáki, 1996; Gong *et al*., 2007); proliferating cell nuclear antigen (PCNA), a cell proliferation marker in the SGZ; FOS, activity-regulated cytoskeleton-associated protein (ARC), and cyclooxygenase-2 (COX2), which are IEG products involved in synaptic plasticity (Chen *et al*., 2002; Guzowski, 2002); ionized calcium-binding adapter molecule 1 (Iba1), a microglia and peripheral macrophage marker in the brain (Jurga *et al*., 2020), cluster of differentiation (CD) 68, which is a marker of activated phagocytic microglia/macrophages and is expressed in both M1-type proinflammatory and M2-type anti-inflammatory microglia/macrophages (Walker and Lue, 2015), and CD163, a M2-type anti-inflammatory microglia/macrophage marker (Jurga *et al*., 2020).

Brain sections were deparaffinized with xylene and subsequently hydrated with ethanol. Then, antigen retrieval treatment was conducted for some of the primary antibodies under the conditions shown in Supplementary Table 1. To quench the endogenous peroxidase, the sections were then incubated in 0.3% (v/v) hydrogen peroxide solution in absolute methanol at room temperature for 30 min. Phosphate-buffered saline (pH 7.4) containing 1.5% normal horse or goat serum was used to block the nonspecific binding of mouse and rabbit primary antibodies at room temperature for 30 min. The sections were incubated with each primary antibody at 4°C overnight, and then with the secondary antibody at room temperature for 30 min. Immunodetection was carried out by using Vectastain® Elite ABC kit (Vector Laboratories Inc, Burlingame, CA, USA) according to the manufacturer's protocol with 3,3'-diaminobenzidine/H_2O_2 in Tris-buffered saline (pH 7.6) as the chromogen. Then the color-developed sections were counterstained with hematoxylin. Immunohistochemistry of each antigen was performed on one section in each animal.

To evaluate apoptosis in the SGZ, a terminal deoxynucleotidyl transferase dNTP nick end labeling (TUNEL) assay was performed using an ApopTag® Peroxidase *In situ* Apoptosis Detection Kit (MilliporeSigma, Burlington, MA, USA) following the manufacturer's instructions with 3,3'-diaminobenzidine/H_2O_2 as a chromogen. One section per animal was subjected to TUNEL assay.

Evaluation of immunoreactive and apoptotic cells

In the brain samples of Day 11, glial cell populations distributed within the DG hilus, i.e., $Iba1^+$, $CD68^+$, $CD163^+$, or $GFAP^+$ cells, were bilaterally counted and normalized per area unit of the whole area of the DG hilus (Supplementary Fig. 2). In the brain samples of Day 38, $GFAP^+$, $SOX2^+$ or $TBR2^+$ cells of granule cell lineages, and $PCNA^+$ proliferating cells in the SGZ of the whole DG area were bilaterally counted and normalized for the length of the SGZ (Supplementary Fig. 2). DCX^+, $TUBB3^+$, or $NeuN^+$

Table 1. Transcript-level expression changes in the hippocampal dentate gyrus on acute phase (Day 11).

	Ctrl		LPS alone		LPS-AGIQ	
	Relative transcript level normalized to					
	Gapdh	*Hprt1*	*Gapdh*	*Hprt1*	*Gapdh*	*Hprt1*
Oxidative stress-related genes						
Nfe2l2	1.01 ± 0.15	1.00 ± 0.09	1.26 ± 0.33	1.28 ± 0.26*	1.43 ± 0.32	1.33 ± 0.27
Keap1	1.01 ± 0.17	1.00 ± 0.09	1.08 ± 0.15	1.11 ± 0.06*	1.23 ± 0.06	1.14 ± 0.06
Hmox1	1.05 ± 0.31	1.03 ± 0.24	1.44 ± 0.48	1.46 ± 0.40*	1.44 ± 0.43	1.33 ± 0.37
Sod1	1.02 ± 0.21	1.01 ± 0.15	1.03 ± 0.17	1.06 ± 0.06	0.94 ± 0.08	0.87 ± 0.07††
Sod2	1.01 ± 0.18	1.01 ± 0.15	1.14 ± 0.21	1.17 ± 0.19	1.14 ± 0.12	1.06 ± 0.10
Gpx1	1.03 ± 0.28	1.03 ± 0.29	1.20 ± 0.41	1.22 ± 0.34	1.21 ± 0.37	1.12 ± 0.33
Gpx4	1.01 ± 0.17	1.00 ± 0.11	1.05 ± 0.16	1.08 ± 0.05	1.10 ± 0.08	1.02 ± 0.10
Cat	1.01 ± 0.14	1.00 ± 0.07	0.95 ± 0.14	0.98 ± 0.07	1.04 ± 0.03	0.97 ± 0.03
Mt1	1.03 ± 0.26	1.02 ± 0.24	2.01 ± 0.50**	2.05 ± 0.35**	1.90 ± 0.55	1.76 ± 0.47
Mt2a	1.05 ± 0.35	1.04 ± 0.33	1.78 ± 0.38**	1.83 ± 0.29**	1.88 ± 0.68	1.73 ± 0.57
Nos2	1.10 ± 0.41	1.01 ± 0.16	2.63 ± 2.94	2.82 ± 3.58	1.22 ± 0.3	1.15 ± 0.31
Chemical mediator and related marker genes						
Nfkb1	1.01 ± 0.16	1.00 ± 0.10	1.38 ± 0.29*	1.41 ± 0.21**	1.58 ± 0.22	1.46 ± 0.18
Tnf	1.03 ± 0.28	1.01 ± 0.18	1.65 ± 0.42*	1.71 ± 0.47*	1.74 ± 0.74	1.61 ± 0.64
Il1b	1.11 ± 0.46	1.12 ± 0.48	77.33 ± 54.95*	79.75 ± 55.96*	106.66 ± 56.64	97.98 ± 49.44
Il4	1.04 ± 0.31	1.03 ± 0.24	1.27 ± 0.60	1.28 ± 0.54	1.44 ± 0.59	1.33 ± 0.51
Il6	1.04 ± 0.35	1.02 ± 0.24	1.33 ± 0.58	1.34 ± 0.52	1.34 ± 0.59	1.24 ± 0.51
Il10	1.06 ± 0.38	1.03 ± 0.27	1.48 ± 0.57	1.49 ± 0.49	1.51 ± 0.71	1.40 ± 0.62
Tgfb1	1.01 ± 0.18	1.00 ± 0.09	1.74 ± 0.48**	1.76 ± 0.35**	1.65 ± 0.45	1.53 ± 0.40
Astrocyte and microglia marker genes						
Gfap	1.02 ± 0.18	1.00 ± 0.09	1.47 ± 0.37*	1.52 ± 0.35*	1.48 ± 0.17	1.37 ± 0.14
Aif1	1.02 ± 0.23	1.01 ± 0.12	2.65 ± 0.86**	2.68 ± 0.72**	2.65 ± 0.86	2.46 ± 0.80

Abbreviations: AGIQ, alpha-glycosyl isoquercitrin; *Aif1*, allograft inflammatory factor 1 (also known as Iba1: ionized calcium binding adapter molecule 1); *Cat*, catalase; Ctrl, controls; *Gapdh*, glyceraldehyde-3-phosphate dehydrogenase; *Gfap,* glial fibrillary acidic protein; *Gpx1*, glutathione peroxidase 1; *Gpx4*, glutathione peroxidase 4; *Hmox1*, heme oxygenase 1; *Hprt1*, hypoxanthine phosphoribosyltransferase 1; *Il1b*, interleukin 1 beta; *Il4*, interleukin 4; *Il6*, interleukin 6; *Il10*, interleukin 10; *Keap1*, Kelch-like ECH-associated protein 1; LPS, lipopolysaccharides; *Mt1*, metallothionein 1; *Mt2a*, metallothionein 2A; *Nfe2l2*, nuclear factor, erythroid 2-like 2 (also known as NRF2: nuclear factor erythroid 2-related factor 2); *Nfkb1*, nuclear factor kappa B subunit 1; *Nos2*, nitric oxide synthase 2 (also known as iNOS: inducible nitric oxide synthase); *Sod1*, superoxide dismutase 1; *Sod2*, superoxide dismutase 2; *Tgfb1*, transforming growth factor, beta 1; *Tnf*, tumor necrosis factor. Data are expressed as the mean ± SD. $N = 6$/group. *$P < 0.05$, **$P < 0.01$, significantly different from the controls by Student's *t*-test or Aspin–Welch's *t*-test. ††$P < 0.01$, significantly different from the LPS-alone group by Student's *t*-test or Aspin–Welch's *t*-test.

cells of granule cell lineages distributed in the SGZ and GCL, and FOS$^+$, ARC$^+$, or COX2$^+$ granule cells in the whole GCL area were bilaterally counted and normalized for the length of the SGZ. TUNEL$^+$ apoptotic cells counted in the SGZ were similarly normalized for the length of the SGZ. All the GABAergic interneuron subpopulations distributed within the hilus of the DG, i.e., PVALB$^+$, RELN$^+$, CALB2$^+$, GAD67$^+$, or SST$^+$ cells, were bilaterally counted and normalized per area unit of the hilar area. Immunoreactive neurons located inside of the Cornu Ammonis region 3, consisting of large pyramidal neurons were excluded from the counting in the hilus of the DG. The number of each immunoreactive cell population except for NeuN$^+$ cells was manually counted while blinded to the treatment conditions under microscopic observation using a BX51 microscope (Olympus Corporation, Tokyo, Japan). In the case of the counting of NeuN$^+$ cells, digital photomicrographs at 200-fold magnification were taken using a BX51 microscope attached to a DP27 Digital Camera System (Olympus Corporation), and the immunoreactive cells were counted automatically applying the WinROOF image analysis software package (version 5.7; Mitani Corporation, Fukui, Japan). The length of the SGZ and the area of the DG hilus were measured by cellSens image analysis software package (standard package 1.9; Olympus Corporation).

Gene expression analysis

Expression levels of mRNA in the hippocampal DG were examined using real-time reverse transcription-PCR. From the methacarn-fixed brain tissues, 2-mm-thick coronal cerebral slices were prepared at the position of −3.0 mm from the bregma. Tissues of the hippocampal DG were collected from the slice using punch-biopsy devices with a bore size of 1-mm-diameter (Kai Industries Co., Ltd., Gifu, Japan). Total RNA was extracted from tissue samples from 6 animals of each group using QIAzol (Qiagen, Hilden, Germany) and RNeasy Mini kit (Qiagen). First-strand cDNA was synthesized using SuperScript® III Reverse Transcriptase (Thermo Fisher Scientific). Analysis of the transcript levels for gene targets shown in Supplementary Table 2 was performed using the PCR primers designed with Primer Express software (Version 3.0; Thermo Fisher Scientific) or Primer-BLAST (NCBI, https://www.ncbi.nlm.nih.gov/tools/primer-blast/); however, only the primer sequences of *Il6* were the same as those used in a previous report (Ghowsi *et al*., 2018). Real-time PCR with Power SYBR® Green PCR Master Mix (Thermo Fisher Scientific) was conducted using a StepOnePlus™ Real-time PCR System (Thermo Fisher Scientific). The relative differences in gene expression between three groups were calculated using threshold cycle (C_T) values that were first normalized to those of the glyceraldehyde-3-phosphate dehydrogenase gene (*Gapdh*) or hypoxanthine phosphoribosyltransferase 1 gene (*Hprt1*) as the endogenous control gene in the same sample and then relative to a control C_T value using the $2^{-\Delta\Delta C_T}$ method (Livak and Schmittgen, 2001).

Statistical analysis

Numerical data were expressed as the mean ± SD. The statistical significance of differences between groups was evaluated as follows.

To evaluate the effect of LPS exposure, comparisons were made between the controls and LPS-alone group; to evaluate the impact of AGIQ treatment, comparisons were made between the LPS-alone and LPS-AGIQ groups. Data were analyzed by Levene's test for homogeneity of variance. If the variance was homogenous between the groups, Student's *t*-test was applied, and Aspin–Welch's *t*-test was performed when the variance was heterogeneous. All analyses were performed using the IBM SPSS Statistics ver. 25 (International Business Machines Corporation, Armonk, NY, USA), and $P < 0.05$ was considered statistically significant.

RESULTS

In life parameter data and necropsy data

Over the period from Day 9 to Day 22 after LPS treatment, the body weight of the LPS-alone group was significantly decreased compared with the controls (Supplementary Fig. 3), and the food and water consumption from Day 9 to Day 11 were also decreased significantly. While comparing with the controls, the food consumption in the LPS-alone group from Day 25 to Day 33 was significantly increased, and the water consumption was increased on Day 25. Compared with the LPS-alone group, food consumption on Day 4, Day 22 and Day 33 was significantly decreased and water consumption on Day 10 was significantly increased in the LPS-AGIQ group, but body weight was not significantly different between the two groups throughout the study period.

With regard to the body weight at the necropsy, the LPS-alone group was significantly lower on Day 11 than the controls, but there was no significant difference on Day 38 between the two groups (Supplementary Table 3). There were no significant differences between the LPS-alone and LPS-AGIQ groups at any necropsy days. With regard to the brain weight on Day 38, there were no significant differences between the controls and LPS-alone group, or between the LPS-alone and LPS-AGIQ groups (Supplementary Table 3).

The LPS-administered animals had high incidence of reddish tear from 1 to 3 days after LPS administration. No abnormalities in the gait and behaviors were observed in any group before necropsy.

Average AGIQ intake in the LPS-AGIQ group was 373.5 ± 18.9 mg/kg body weight/day.

Behavioral test

Open field test

There were no significant differences in total moving distance and center region rate between the controls and LPS-alone group, or between the LPS-alone and LPS-AGIQ groups (Fig. 2A, Supplementary Table 4).

Contextual fear conditioning test

The freezing rate of the LPS-alone group was significantly decreased as compared with the controls at the fear acquisition trial (Fig. 2B, Supplementary Table 5). In addition, compared with LPS-alone group, the LPS-AGIQ group had a tendency of high freezing rate, but there was no significant difference. On the other hand, there was no significant difference in the relative freezing rate in the 3rd–5th trials of extinction learning between the controls and LPS-alone group, and between the LPS-

Table 2. Transcript-level expression changes in the hippocampal dentate gyrus on chronic phase (Day 38).

	Ctrl		LPS alone		LPS-AGIQ	
	Relative transcript level normalized to					
	Gapdh	*Hprt1*	*Gapdh*	*Hprt1*	*Gapdh*	*Hprt1*
Granule cell lineage marker genes						
Nes	1.04 ± 0.33	1.03 ± 0.31	1.10 ± 0.23	1.04 ± 0.21	0.91 ± 0.18	0.87 ± 0.17
Sox2	1.03 ± 0.26	1.02 ± 0.23	1.22 ± 0.30	1.16 ± 0.31	1.00 ± 0.21	0.94 ± 0.16
Eomes	1.07 ± 0.39	1.05 ± 0.35	2.31 ± 1.20*	2.08 ± 0.71**	2.07 ± 0.69	1.96 ± 0.60
Dcx	1.01 ± 0.16	1.01 ± 0.15	1.33 ± 0.32*	1.22 ± 0.11*	1.13 ± 0.12	1.07 ± 0.07†
Tubb3	1.01 ± 0.16	1.00 ± 0.09	1.13 ± 0.23	1.05 ± 0.15	0.98 ± 0.05	0.94 ± 0.12
Dpysl3	1.01 ± 0.13	1.00 ± 0.09	1.17 ± 0.36	1.07 ± 0.17	1.04 ± 0.11	1.00 ± 0.18
Rbfox3	1.02 ± 0.19	1.01 ± 0.12	0.92 ± 0.19	0.86 ± 0.15	1.01 ± 0.22	0.98 ± 0.32
GABAergic interneuron marker genes						
Calb1	1.03 ± 0.31	1.02 ± 0.22	1.49 ± 0.63	1.34 ± 0.44	1.67 ± 0.65	1.64 ± 0.73
Calb2	1.01 ± 0.15	1.01 ± 0.12	1.53 ± 0.68	1.39 ± 0.50	1.00 ± 0.10	0.96 ± 0.19
Pvalb	1.04 ± 0.29	1.02 ± 0.23	0.94 ± 0.31	0.90 ± 0.36	1.04 ± 0.16	0.99 ± 0.15
Reln	1.03 ± 0.29	1.02 ± 0.23	1.40 ± 0.28*	1.29 ± 0.08*	1.41 ± 0.12	1.34 ± 0.16
Sst	1.03 ± 0.29	1.02 ± 0.20	1.35 ± 0.20	1.28 ± 0.31	1.47 ± 0.28	1.40 ± 0.32
Neurotrophic factor-related genes						
Bdnf	1.01 ± 0.18	1.01 ± 0.16	1.08 ± 0.26	0.99 ± 0.10	1.10 ± 0.12	1.06 ± 0.17
Ntrk2	1.03 ± 0.28	1.02 ± 0.24	1.26 ± 0.22	1.18 ± 0.15	1.17 ± 0.14	1.11 ± 0.10
Cell proliferation marker gene						
Pcna	1.02 ± 0.19	1.01 ± 0.12	1.47 ± 0.40*	1.35 ± 0.18**	1.16 ± 0.18	1.10 ± 0.07††
Synaptic plasticity-related IEGs						
Arc	1.04 ± 0.35	1.04 ± 0.32	0.91 ± 0.20	0.85 ± 0.15	1.34 ± 0.52	1.32 ± 0.62
Fos	1.02 ± 0.22	1.01 ± 0.18	1.41 ± 0.61	1.28 ± 0.41	1.22 ± 0.27	1.17 ± 0.33
Ptgs2	1.02 ± 0.22	1.01 ± 0.17	0.98 ± 0.29	0.90 ± 0.17	1.13 ± 0.32	1.09 ± 0.37
Glutamate receptor and transporter genes						
Gria1	1.03 ± 0.29	1.03 ± 0.26	1.10 ± 0.47	1.01 ± 0.38	1.32 ± 0.37	1.28 ± 0.44
Gria2	1.04 ± 0.33	1.04 ± 0.30	1.09 ± 0.42	1.00 ± 0.33	1.31 ± 0.40	1.27 ± 0.47
Gria3	1.05 ± 0.34	1.04 ± 0.32	1.11 ± 0.38	1.02 ± 0.29	1.33 ± 0.33	1.29 ± 0.41
Grin2a	1.08 ± 0.48	1.07 ± 0.45	0.86 ± 0.37	0.79 ± 0.30	1.13 ± 0.39	1.10 ± 0.45
Grin2b	1.05 ± 0.36	1.04 ± 0.32	1.10 ± 0.53	1.02 ± 0.45	1.34 ± 0.37	1.31 ± 0.47
Grin2d	1.03 ± 0.30	1.03 ± 0.27	1.29 ± 0.31	1.20 ± 0.21	1.28 ± 0.26	1.24 ± 0.35
Slc17a6	1.10 ± 0.47	1.08 ± 0.43	1.97 ± 0.95	1.79 ± 0.67	2.17 ± 0.86	2.11 ± 0.93
Slc17a7	1.01 ± 0.12	1.00 ± 0.07	1.03 ± 0.27	0.95 ± 0.16	1.08 ± 0.12	1.04 ± 0.18
Cholinergic receptor genes						
Chrna7	1.01 ± 0.18	1.01 ± 0.13	1.04 ± 0.26	0.96 ± 0.17	1.22 ± 0.34	1.18 ± 0.42
Chrnb2	1.02 ± 0.19	1.00 ± 0.10	1.04 ± 0.20	0.96 ± 0.05	1.16 ± 0.37	1.13 ± 0.44

Abbreviations: AGIQ, alpha-glycosyl isoquercitrin; *Arc*, activity-regulated cytoskeleton-associated protein; *Bdnf*, brain-derived neurotrophic factor; *Calb1*, calbindin 1 (also known as calbindin-D-28K); *Calb2*, calbindin 2 (also known as calbindin-D-29K and calretinin); *Chrna7*, cholinergic receptor nicotinic alpha 7 subunit; *Chrnb2*, cholinergic receptor nicotinic beta 2 subunit; Ctrl, controls; *Dcx*, doublecortin; *Dpysl3,* dihydropyrimidinase-like 3; *Eomes,* eomesodermin (also known as TBR2: T-box brain protein 2); *Fos*, Fos proto-oncogene, AP-1 transcription factor subunit; GABA, γ-aminobutyric acid; *Gapdh*, glyceraldehyde-3-phosphate dehydrogenase; *Gria1*, glutamate ionotropic receptor AMPA type subunit 1; *Gria2*, glutamate ionotropic receptor AMPA type subunit 2; *Gria3*, glutamate ionotropic receptor AMPA type subunit 3; *Grin2a*, glutamate ionotropic receptor NMDA type subunit 2A; *Grin2b*, glutamate ionotropic receptor NMDA type subunit 2B; *Grin2d*, glutamate ionotropic receptor NMDA type subunit 2D; *Hprt1*, hypoxanthine phosphoribosyltransferase 1; IEG, immediate-early gene; LPS, lipopolysaccharides; *Nes*, nestin; *Ntrk2*, neurotrophic receptor tyrosine kinase 2 (also known as TrkB: tropomyosin receptor kinase B); *Pcna*, proliferating cell nuclear antigen; *Ptgs2*, prostaglandin-endoperoxide synthase 2; *Pvalb*, parvalbumin; *Rbfox3*, RNA binding fox-1 homolog 3 (also known as NeuN); *Reln*, reelin; *Slc17a6*, solute carrier family 17 member 6; *Slc17a7*, solute carrier family 17 member 7; *Sox2*, SRY-box transcription factor 2; *Sst*, somatostatin; *Tubb3*, tubulin, beta 3 class III. Data are expressed as the mean ± SD. $N = 6$/group. *$P < 0.05$, **$P < 0.01$, significantly different from the controls by Student's *t*-test or Aspin–Welch's *t*-test. $^{\dagger}P < 0.05$, $^{\dagger\dagger}P < 0.01$, significantly different from the LPS-alone group by Student's *t*-test or Aspin–Welch's *t*-test.

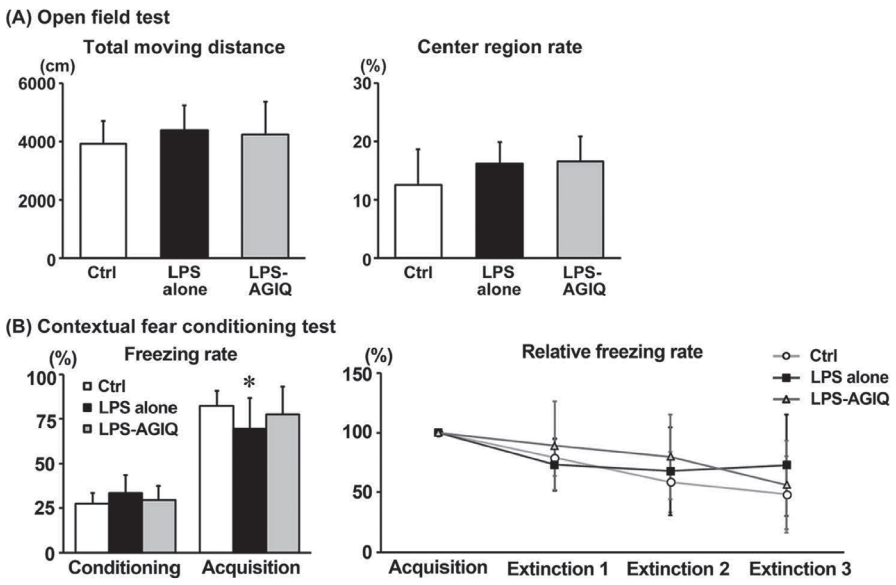

Fig. 2. Parameters for behavior tests as (A) open field test at Day 31 and Day 32 or (B) contextual fear conditioning test from Day 34 to Day 38 of the experiment after lipopolysaccharides (LPS) exposure at Day 8 and Day 10 and α-glycosyl isoquercitrin (AGIQ) exposure throughout the experimental period. For the open field test, total moving distance and center region rate were shown as indices of locomotor activity and anxiolytic behavior, respectively. For the contextual fear conditioning test, freezing rate of 2nd trial and relative freezing rate of 3rd trial, 4th trial, and 5th trial (each freezing rate/freezing rate of 2nd trial) were shown as indices of fear memory acquisition and fear extinction learning, respectively. Data are expressed as the mean + SD or mean ± SD. $N = 10$/group. *$P < 0.05$, significantly different from the controls (Ctrl) by Student's *t*-test or Aspin–Welch's *t*-test.

alone and LPS-AGIQ groups (Fig. 2B).

Proinflammatory cytokine and MDA levels in the brain

Proinflammatory cytokine levels

On Day 11, the level of IL-1β in the hippocampus, and the levels of IL-1β and TNF-α in the cerebral cortex were significantly increased in the LPS-alone group compared with the controls, and an increasing trend of TNF-α level in the hippocampus was shown in the LPS-alone group (Fig. 3A–C). However, the LPS-AGIQ group showed a decreasing trend of IL-1β level and a significant decrease of TNF-α level in both the hippocampus and cerebral cortex compared with the LPS-alone group. No significant difference was found in the level of IL-6 in the hippocampus or cerebral cortex between the controls and LPS-alone group, as well as between the LPS-alone and LPS-AGIQ groups.

MDA levels

There was no significant difference in the level of MDA between the controls and LPS-alone group in either of the hippocampus or cerebral cortex (Fig. 3D). The level of MDA in the hippocampus and cerebral cortex of the LPS-AGIQ group was significantly increased compared with the LPS-alone group.

Numbers of immunoreactive cells and apoptotic cells in the DG

Numbers of glial cell populations in the DG hilus

On Day 11, the numbers of $CD68^+$ and $Iba1^+$ microglia/macrophages, and $GFAP^+$ astrocytes were significantly increased in the LPS-alone group compared with the controls (Fig. 4). Regarding the number of $CD163^+$ microglia/macrophages, there was no significant difference between the controls and LPS-alone group. On the other hand, the LPS-AGIQ group did not show any significant difference in the numbers of these glial cell populations compared with the LPS-alone group. However, the number of $CD68^+$ microglia/macrophages in the LPS-AGIQ group tended to decrease and the number of $CD163^+$ microglia/macrophages cells tended to increase compared with the LPS-alone group.

Numbers of granule cell lineage subpopulations in the SGZ and/or GCL

On Day 38, the number of DCX^+ cells in the LPS-

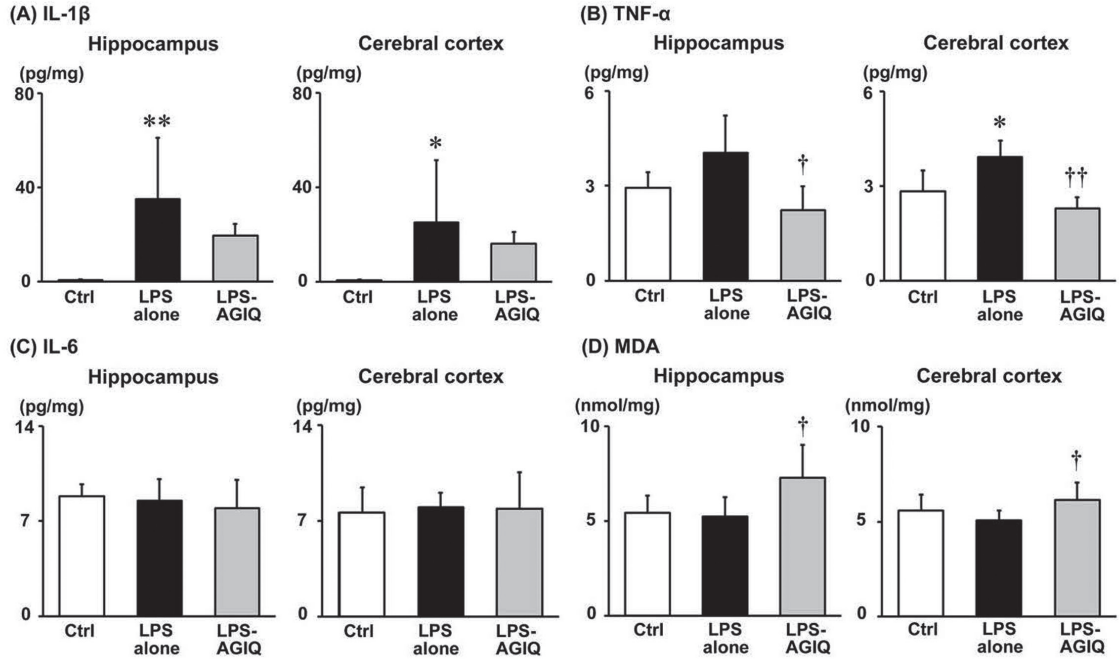

Fig. 3. Proinflammatory cytokine levels of (A) interleukin (IL)-1β, (B) tumor necrosis factor (TNF)-α, or (C) IL-6, and (D) level of malondialdehyde (MDA) as an oxidative stress marker in the hippocampus and cerebral cortex at Day 11 of the experiment after lipopolysaccharides (LPS) exposure at Day 8 and Day 10 and α-glycosyl isoquercitrin (AGIQ) exposure throughout the experimental period. Data are expressed as the mean + SD. $N = 6$/group. $^{*}P < 0.05$, $^{**}P < 0.01$, significantly different from the controls (Ctrl) by Student's *t*-test or Aspin–Welch's *t*-test. $^{\dagger}P < 0.05$, $^{\dagger\dagger}P < 0.01$, significantly different from the LPS-alone group by Student's *t*-test or Aspin–Welch's *t*-test.

alone group was significantly lower than that in the controls (Fig. 5, Supplementary Fig. 4). On the other hand, there were no significant differences in the numbers of $GFAP^+$ cells, $SOX2^+$ cells, $TBR2^+$ cells, $TUBB3^+$ cells, and $NeuN^+$ cells between the controls and LPS-alone group. The numbers of immunoreactive cells for all granule cell lineage markers examined did not show any significant difference between the LPS-alone and LPS-AGIQ groups.

Cell proliferation activity and apoptotic cell numbers in the SGZ

On Day 38, there were no significant differences in the numbers of $PCNA^+$ proliferating cells and $TUNEL^+$ apoptotic cells between the controls and LPS-alone group (Fig. 5, Supplementary Fig. 5). However, the number of $PCNA^+$ cells significantly increased in the LPS-AGIQ group compared with the LPS-alone group.

Numbers of immunoreactive cells for synaptic plasticity-related IEG products in the GCL

On Day 38, the number of FOS^+ cells in the LPS-alone group was significantly decreased compared with the controls, and the number of $COX2^+$ cells showed a decreasing trend compared with the controls (Fig. 5, Supplementary Fig. 6). On the other hand, the numbers of FOS^+ cells and $COX2^+$ cells in the LPS-AGIQ group were significantly increased compared with the LPS-alone group. Regarding the number of ARC^+ cells, there were no significant differences between the controls and LPS-alone group and between the LPS-alone and LPS-AGIQ groups.

Numbers of interneuron subpopulations in the DG hilus

On Day 38, there were no significant differences in the numbers of $PVALB^+$ cells, $RELN^+$ cells, $CALB2^+$ cells, $GAD67^+$ cells, and SST^+ cells between the controls and LPS-alone group (Supplementary Fig. 7). The number of $CALB2^+$ cells in the LPS-AGIQ group was significantly increased compared with the LPS-alone group (Fig. 5, Supplementary Fig. 7). No significant differences were shown in the numbers of $PVALB^+$ cells, $RELN^+$ cells, $GAD67^+$ cells, and SST^+ cells between the LPS-alone and LPS-AGIQ groups.

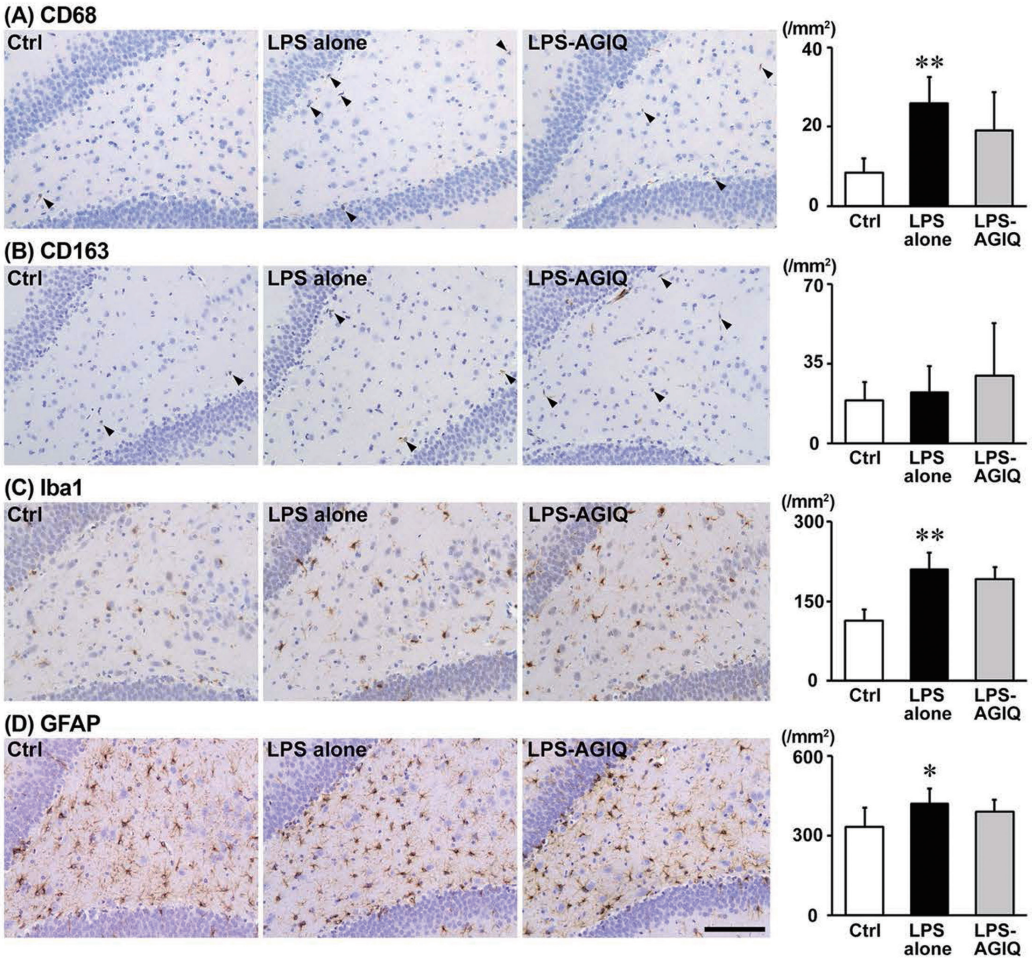

Fig. 4. Distribution of immunoreactive cells for glial cell marker proteins, i.e., (A) cluster of differentiation (CD) 68, (B) CD163, (C) ionized calcium-binding adapter molecule 1 (Iba1), and (D) glial fibrillary acidic protein (GFAP) in the hilus of the hippocampal dentate gyrus (DG) at Day 11 of the experiment after lipopolysaccharides (LPS) exposure at Day 8 and Day 10 and α-glycosyl isoquercitrin (AGIQ) exposure throughout the experimental period. Representative images from the controls, and LPS-alone and LPS-AGIQ groups (in order from left to right). Arrowheads indicate immunoreactive cells. Magnification × 200; bar 100 μm. Graphs show the number of immunoreactive cells in the DG hilus. Values are expressed as the mean + SD. $N = 8$/group. *$P < 0.05$, **$P < 0.01$, significantly different from the controls (Ctrl) by Student's *t*-test or Aspin–Welch's *t*-test.

Transcript-level expression changes in the hippocampal DG

On Day 11, the transcript levels of *Nfe2l2, Keap1, Hmox1, Mt1*, and *Mt2a* among oxidative stress-related genes were significantly increased in the LPS-alone group after normalization with *Gapdh* and/or *Hprt1* compared with the controls (Table 1). The transcript level of *Sod1* in the LPS-AGIQ group was significantly decreased after normalization with *Hprt1* compared with the LPS-alone group. With regard to genes encoding chemical mediator and related marker genes, the transcript levels of *Nfkb1*, *Tnf*, *Il1b*, and *Tgfb1* were significantly increased after normalization with *Gapdh* and *Hprt1* in the LPS-alone group compared with the controls. The transcript levels of *Gfap* and *Aif1* among astrocyte and microglia marker genes were significantly increased in the LPS-alone group after normalization with *Gapdh* and *Hprt1* compared with the controls. However, chemical mediator and related marker genes and astrocyte and microglia marker genes did not show any significant differences between the LPS-AGIQ and LPS-alone groups.

On Day 38, the transcript levels of *Eomes* and *Dcx* among

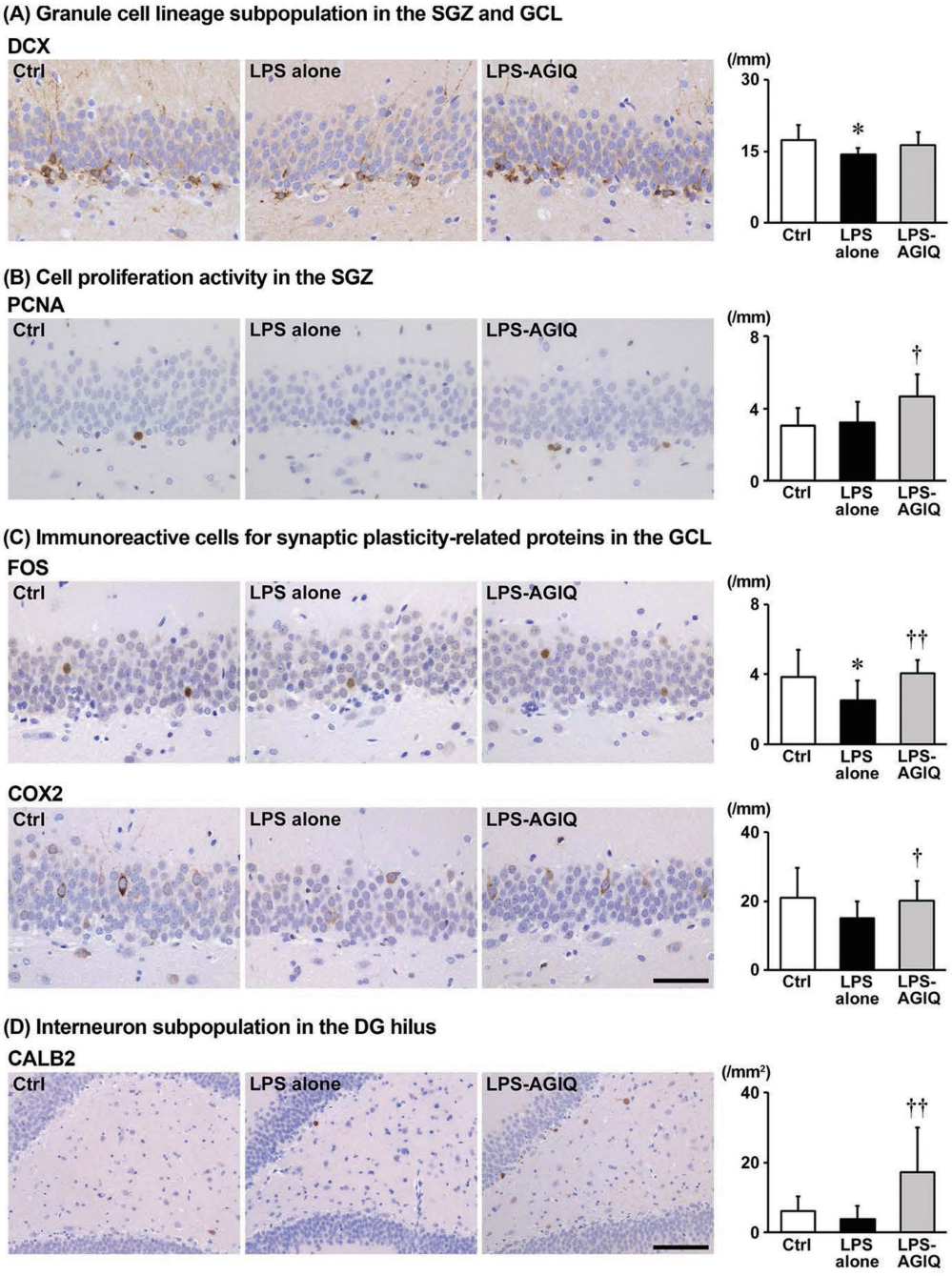

Fig. 5. Distribution of immunoreactive cells for (A) doublecortin (DCX) as a granule cell lineage marker in the subgranular zone (SGZ) and granule cell layer (GCL), (B) proliferating cell nuclear antigen (PCNA) as a cell proliferation marker in the SGZ, (C) Fos proto-oncogene, AP-1 transcription factor subunit (FOS), or cyclooxygenase-2 (COX2) as a synaptic plasticity-related immediate-early gene product in the GCL, and (D) calbindin-D-29K (CALB2) as a γ-aminobutyric acid (GABA)-ergic interneuron marker in the hilus of the dentate gyrus (DG) at Day 38 of the experiment after lipopolysaccharides (LPS) exposure at Day 8 and Day 10 and α-glycosyl isoquercitrin (AGIQ) exposure throughout the experimental period. Representative images from the controls, and LPS-alone and LPS-AGIQ groups (in order from left to right). Magnification × 400 (A–C), × 200 (D); bar 50 μm (A–C), 100 μm (D). Graphs show the number of immunoreactive cells in the SGZ and/or GCL (A–C) or DG hilus (D). Values are expressed as the mean + SD. $N = 10$/group. *$P < 0.05$, significantly different from the controls (Ctrl) by Student's *t*-test or Aspin–Welch's *t*-test. †$P < 0.05$, ††$P < 0.01$, significantly different from the LPS-alone group by Student's *t*-test or Aspin–Welch's *t*-test.

granule cell lineage marker genes were significantly increased in the LPS-alone group after normalization with *Gapdh* and *Hprt1* compared with the controls, and the transcript level of *Dcx* was significantly decreased in the LPS-AGIQ group after normalization with *Hprt1* compared with the LPS-alone group (Table 2). Regarding the GABAergic interneuron marker genes, the transcript level of *Reln* was significantly increased after normalization with *Gapdh* and *Hprt1* in the LPS-alone group compared with the controls, but there was no significant difference in the *Reln* transcript level between the LPS-alone and LPS-AGIQ groups. The transcript level of *Pcna*, a cell proliferation marker gene, was significantly increased in the LPS-alone group after normalization with *Gapdh* and *Hprt1* compared with the controls and was significantly decreased in the LPS-AGIQ group after normalization with *Hprt1* compared with the LPS-alone group. The transcript levels of neurotrophic factor-related genes, synaptic plasticity-related IEGs, glutamate receptor and transporter genes, and cholinergic receptor genes did not show any statistically significant differences between the controls and LPS-alone group, and between the LPS-alone and LPS-AGIQ groups.

DISCUSSION

Rats exposed to LPS reportedly exhibit depression-like behavior with neuroinflammation (Zhang *et al*., 2019; Salmani *et al*., 2018). However, this study showed no evidence of depression-like behaviors, i.e., decreased spontaneous locomotor activity and enhanced anxiety-like behavior, in the open-field test after LPS administration. Most of the depression-like behaviors resulting from LPS exposure were observed soon after the LPS administration (Boldrini *et al*., 2018; Wang *et al*., 2020). In the present study, the behavioral tests were performed 3 weeks after LPS exposure, so the depression-like behaviors may have disappeared following the subsiding of acute inflammation. On the other hand, we observed that LPS exposure reduced freezing rate at the fear acquisition trial, and that AGIQ treatment had a trend toward recovery of the LPS-induced impairment of fear memory acquisition. It is reported that LPS-induced neuroinflammation impairs context discrimination memory by disrupting cellular pattern separation processes within the hippocampus, thus linking acute neuroinflammation to disruption of specific neural circuit functions and cognitive impairment (Czerniawski and Guzowski, 2014). We recently found that continuous exposure to AGIQ from the embryonic age facilitated fear extinction learning in a contextual fear conditioning test and an increase in the number of FOS^+ granule cells in the hippocampal DG, suggesting increased synaptic plasticity for facilitation of fear memory extinction (Okada *et al*., 2019). In contrast to the AGIQ function to facilitate fear memory extinction on normal animals, the present study results suggest that AGIQ may ameliorate impairment of fear memory acquisition in neuroinflammation-loaded animals by improving neural circuit function in the hippocampus. Therefore, we further investigated the involvement of neuroinflammation, oxidative stress, and adult neurogenesis in the hippocampus in LPS-induced impairment of learning and memory using biochemical, immunohistochemical, and gene expression analyses.

On the next day of the last LPS administration, we found increased levels of IL-1β and TNF-α as proinflammatory cytokines in the hippocampus and cerebral cortex of animals treated with LPS alone. At the same time, these animals upregulated expressions of *Il1b* and *Tnf*, encoding IL-1β and TNF-α, respectively, in the hippocampal DG with upregulation of *Nfkb1*, encoding a key transcription factor NFκB that controls the expression of proinflammatory cytokines, including IL-1β and TNF-α (Ponnappan, 1998). At the same time point after LPS administration, the number of $Iba1^+$ microglia/macrophages was increased in the DG hilus, accompanied by upregulation of *Aif1*, encoding Ibal. Additionally, the number of $CD68^+$ microglia/macrophages was also increased in these animals, whereas the number of $CD163^+$ microglia/macrophages was unaltered. CD68 is mainly expressed in activated microglia/macrophages, including both proinflammatory M1-type and anti-inflammatory M2-type, whereas CD163 is expressed in M2-type microglia/macrophages (Jurga *et al*., 2020; Walker and Lue, 2015). Thus, our results indicated that the increases in the number of $Iba1^+$ and $CD68^+$ microglia/macrophages following LPS administration reflect an increase in the number of proinflammatory M1-type microglia/macrophages. IL-1β and TNF-α are mainly produced by M1-type microglia/macrophages (Jurga *et al*., 2020). Thus, the increase in the levels of these proinflammatory cytokines in the hippocampus also supports our interpretation. As a result of LPS administration, the number of $GFAP^+$ astrocytes was also increased in the DG hilus in accordance with upregulation of *Gfap* as an astrocyte marker gene. M1-type microglia induce reactive astrocytes by producing proinflammatory cytokines during neuroinflammation (Liddelow *et al*., 2017) and reactive astrocytes express GFAP more highly than dormant astrocytes (Spanos and Liddelow, 2020). These findings indicated that LPS activated M1-type microglia followed by an increased number of reactive astrocytes in the hippocampus. In this study, AGIQ

treatment suppressed the increased proinflammatory cytokine levels such as TNF-α in the hippocampus and cerebral cortex induced by LPS administration, while transcript levels of chemical mediator and related marker genes did not respond to the AGIQ treatment. AGIQ-treated animals also showed a decreasing tendency in the number of $CD68^+$ cells and an increasing tendency in the number of $CD163^+$ cells in the DG hilus, suggesting a reduced number of M1-type proinflammatory microglia/macrophages and an increased number of M2-type anti-inflammatory microglia/macrophages. These results indicate that LPS exposure induced neuroinflammation that could be partially prevented by AGIQ treatment.

Systemic LPS exposure and neuroinflammation increase oxidative stress in brain regions such as the hippocampus (Jamali-Raeufy *et al*., 2021). In the present study, we had no evidence of increased oxidative stress, i.e., increased level of MDA, in the hippocampus and cerebral cortex on the next day of the last LPS administration, while upregulation in the transcript level was observed in several oxidative stress-related genes. On the other hand, AGIQ treatment unexpectedly increased MDA levels in the hippocampus and cerebral cortex accompanying downregulation of *Sod1*. These results may be related to the AGIQ dosing regimen in this study, which started one week before LPS administration. Because of the antioxidant properties of AGIQ, pretreatment of naïve rats with AGIQ may have reduced basal level of oxidative stress, accompanied by suppression of antioxidant defense mechanisms. Therefore, LPS administration resulted in temporarily higher levels of oxidative stress in the animals with AGIQ pretreatment than in the animals without AGIQ pretreatment.

Three weeks after the last LPS administration, the number of DCX^+ cells was decreased in the SGZ and GCL of the animals treated with LPS alone. DCX was expressed mainly in type-3 NPCs, but also in type-2b NPCs and immature granule cells (Kempermann *et al*., 2015). However, LPS administration did not change the numbers of other granule cell lineage subpopulations, such as $GFAP^+$ cells (type-1 NSCs), $TBR2^+$ cells as type-2b NPCs, $TUBB3^+$ cells as mainly immature granule cells, and $NeuN^+$ cells as postmitotic immature and mature granule cells (Sibbe and Kulik, 2017; von Bohlen Und Halbach, 2007), suggesting that LPS specifically decreased the number of type-3 NPCs. Neuroinflammation and oxidative stress inhibit adult hippocampal neurogenesis by reducing DCX^+ cells in the SGZ (Bassani *et al*., 2018). However, there were no changes in the number of $PCNA^+$ proliferating cells and $TUNEL^+$ apoptotic cells in the SGZ after LPS administration. These results suggest that the decreased number of type-3 NPCs induced by LPS administration was not caused by a suppression of cell proliferation or an increase in apoptosis, but is due to an inhibition of differentiation of type-2b NPCs to type-3 NPCs.

Although the distribution of GABAergic interneuron subpopulations in the DG hilus was not altered in the LPS-alone group, *Reln* was upregulated in the transcript level in the hippocampal DG. Overexpression of RELN promotes adult neurogenesis and increases the number of DCX^+ cells in the hippocampus of mice (Pujadas *et al*., 2010). Therefore, the upregulated *Reln* expression by LPS administration may be a compensatory response to the reduced number of type-3 NPCs. Additionally, the animals treated with LPS alone also showed upregulated expression of *Eomes*, encoding TBR2, and *Dcx*, supporting the presence of the compensatory response. On the other hand, AGIQ treatment increased the number of $PCNA^+$ SGZ cells and showed an increasing tendency of DCX^+ cells in the SGZ and GCL as compared with LPS alone. Considering that the upregulated *Reln* expression by LPS administration was maintained by AGIQ treatment, AGIQ might promote the proliferation of NPCs to increase the DCX^+ cells. AGIQ treatment also increased the number of $CALB2^+$ interneurons in the DG hilus. In the hippocampal DG, GABAergic interneurons expressing CALB2 regulate other GABAergic interneuron subpopulations, which innervate granule cells through inter-synaptic connections, to regulate the overall hippocampal activity (Gulyás *et al*., 1996). Therefore, the increased number of $CALB2^+$ interneurons in this study was suggested to be a change associated with the promotion of NPC proliferation by AGIQ. These results suggest that AGIQ promotes hippocampal neurogenesis and ameliorates disrupted hippocampal neurogenesis induced by LPS. Moreover, we found that the expressions of *Dcx* and *Pcna* in the AGIQ-treated animals were downregulated to the same level as that in the controls, suggesting that AGIQ sufficiently ameliorated LPS-disrupted hippocampal neurogenesis. As previously mentioned, neuroinflammation inhibits adult hippocampal neurogenesis (Bassani *et al*., 2018) and AGIQ prevented LPS-induced neuroinflammation in this study. Therefore, our results suggest that acute inflammation was involved in disrupted hippocampal neurogenesis caused by LPS and that AGIQ exerted the ameliorating effect on the disrupted neurogenesis through its anti-inflammatory effects.

Animals treated with LPS alone showed a decreased number of FOS^+ granule cells and a decreasing trend in the number of $COX2^+$ granule cells 28 days after the last LPS administration. IEGs including *Fos* and *Ptgs2*, encoding

FOS and COX2, respectively, induce expression immediately after active neural stimulation and play a key role in synaptic plasticity and memory consolidation (Minatohara *et al*., 2016). FOS is a member of the AP-1 family of transcription factors and is involved in stabilizing the storage of experience into long-term memory by neural circuits in the hippocampus (Guzowski *et al*., 2005). A study showed that *Fos* knock-out mice exhibited impaired spatial and contextual long-term memory (Fleischmann *et al*., 2003). COX2 is involved in synaptic plasticity by regulating prostaglandin E_2 signaling, and is also a key player in neuroinflammation (Chen *et al*., 2002). Inhibition or enhancement of COX2 alters excitatory glutamatergic neurotransmission and long-term potentiation (Li *et al*., 2018). Therefore, our results suggest that LPS suppresses synaptic plasticity in hippocampal granule cells after acute inflammation. In contrast, animals treated with both LPS and AGIQ had the same levels of the number of FOS^+ and $COX2^+$ granule cells as the controls, suggesting that AGIQ ameliorates LPS-induced suppression of synaptic plasticity in the granule cells. These findings suggest that synaptic plasticity in the granule cells is involved in both of the disruptive effect of LPS and the ameliorating effect of AGIQ on fear memory acquisition learning. In addition, newborn granule cells from the neurogenic niche are incorporated into hippocampal neural circuits and play an important role in the reconstruction of neural networks, i.e., synaptic plasticity, which is necessary for memory and learning (Miller and Sahay, 2019). In the present study, AGIQ improved LPS-induced suppression of hippocampal neurogenesis and reduction of the number of FOS^+ and $COX2^+$ granule cells. Therefore, our results suggest that the suppression of synaptic plasticity by LPS was related to the disruption of neurogenesis and impaired fear memory acquisition. Moreover, chemopreventive effects of AGIQ on these parameters suggest that LPS-induced neuroinflammation triggers impairments in synaptic plasticity, neurogenesis and fear memory acquisition.

In conclusion, in this study, LPS administration induced acute neuroinflammation in rats, confirmed by increased number of inflammatory microglia and increased levels of proinflammatory cytokines. After that the animals showed impaired fear memory acquisition in the fear conditioning test, accompanied by a disruption of hippocampal neurogenesis as shown by a decreased number of type-3 NPCs and by a suppression of FOS- and COX2-mediated synaptic plasticity in granule cells. In contrast, AGIQ exhibited anti-inflammatory effects and ameliorated these LPS-induced adverse effects. These results suggest that neuroinflammation is a key factor in the development of LPS-induced impairment of fear memory acquisition. Therefore, this study suggests that continuous intake of anti-inflammatory compounds such as AGIQ is potentially beneficial in maintaining memory acquisition.

ACKNOWLEDGMENTS

This work was supported by San-Ei Gen F.F.I. Inc., and a Research Fund from Institute of Global Innovation Research, Tokyo University of Agriculture and Technology. The authors thank Yayoi Kohno for her technical assistance in preparing the histological specimens.

Conflict of interest---- Mihoko Koyanagi is employed by a food additive manufacturer whose product lines include AGIQ. Robert R. Maronpot is a scientific consultant at the aforementioned food additive manufacturer. The views and opinions expressed in this article are those of the authors and not necessarily those of their respective employers. Qian Tang, Kazumi Takashima, Wen Zeng, Hiromu Okano, Xinyu Zou, Yasunori Takahashi, Ryota Ojiro, Shunsuke Ozawa, Toshinori Yoshida, and Makoto Shibutani declare that no conflict of interest exist.

REFERENCES

Akane, H., Saito, F., Yamanaka, H., Shiraki, A., Imatanaka, N., Akahori, Y., Morita, R., Mitsumori, K. and Shibutani, M. (2013): Methacarn as a whole brain fixative for gene and protein expression analyses of specific brain regions in rats. J. Toxicol. Sci., **38**, 431-443.

Akiyama, T., Washino, T., Yamada, T., Koda, T. and Maitani, T. (2000): Constituents of Enzymatically Modified Isoquercitrin and Enzymatically Modified Rutin (Extract). Shokuhin Eiseigaku Zasshi, **41**, 54-60.

Bassani, T.B., Bonato, J.M., Machado, M.M., Cóppola-Segovia, V., Moura, E.L., Zanata, S.M., Oliveira, R.M. and Vital, M.A. (2018): Decrease in Adult Neurogenesis and Neuroinflammation Are Involved in Spatial Memory Impairment in the Streptozotocin-Induced Model of Sporadic Alzheimer's Disease in Rats. Mol. Neurobiol., **55**, 4280-4296.

Berg, D.A., Belnoue, L., Song, H. and Simon, A. (2013): Neurotransmitter-mediated control of neurogenesis in the adult vertebrate brain. Development, **140**, 2548-2561.

Beurel, E., Toups, M. and Nemeroff, C.B. (2020): The Bidirectional Relationship of Depression and Inflammation: double Trouble. Neuron, **107**, 234-256.

Boldrini, M., Fulmore, C.A., Tartt, A.N., Simeon, L.R., Pavlova, I., Poposka, V., Rosoklija, G.B., Stankov, A., Arango, V., Dwork, A.J., Hen, R. and Mann, J.J. (2018): Human Hippocampal Neurogenesis Persists throughout Aging. Cell Stem Cell, **22**, 589-599.e5.

Chen, C., Magee, J.C. and Bazan, N.G. (2002): Cyclooxygenase-2 regulates prostaglandin E2 signaling in hippocampal long-term synaptic plasticity. J. Neurophysiol., **87**, 2851-2857.

Czerniawski, J. and Guzowski, J.F. (2014): Acute neuroinflammation impairs context discrimination memory and disrupts pattern sepa-

ration processes in hippocampus. J. Neurosci., **34**, 12470-12480.
Dantzer, R., O'Connor, J.C., Freund, G.G., Johnson, R.W. and Kelley, K.W. (2008): From inflammation to sickness and depression: when the immune system subjugates the brain. Nat. Rev. Neurosci., **9**, 46-56.
Deroche-Gamonet, V., Revest, J.M., Fiancette, J.F., Balado, E., Koehl, M., Grosjean, N., Abrous, D.N. and Piazza, P.V. (2019): Depleting adult dentate gyrus neurogenesis increases cocaine-seeking behavior. Mol. Psychiatry, **24**, 312-320.
Fleischmann, A., Hvalby, O., Jensen, V., Strekalova, T., Zacher, C., Layer, L.E., Kvello, A., Reschke, M., Spanagel, R., Sprengel, R., Wagner, E.F. and Gass, P. (2003): Impaired long-term memory and NR2A-type NMDA receptor-dependent synaptic plasticity in mice lacking c-Fos in the CNS. J. Neurosci., **23**, 9116-9122.
Freund, T.F. and Buzsáki, G. (1996): Interneurons of the hippocampus. Hippocampus, **6**, 347-470.
Fujii, Y., Kimura, M., Ishii, Y., Yamamoto, R., Morita, R., Hayashi, S.M., Suzuki, K. and Shibutani, M. (2013): Effect of enzymatically modified isoquercitrin on preneoplastic liver cell lesions induced by thioacetamide promotion in a two-stage hepatocarcinogenesis model using rats. Toxicology, **305**, 30-40.
Gárate, I., García-Bueno, B., Madrigal, J.L., Bravo, L., Berrocoso, E., Caso, J.R., Micó, J.A. and Leza, J.C. (2011): Origin and consequences of brain Toll-like receptor 4 pathway stimulation in an experimental model of depression. J. Neuroinflammation, **8**, 151.
Gasparotto Junior, A., Gasparotto, F.M., Lourenço, E.L., Crestani, S., Stefanello, M.E., Salvador, M.J., da Silva-Santos, J.E., Marques, M.C. and Kassuya, C.A. (2011): Antihypertensive effects of isoquercitrin and extracts from Tropaeolum majus L.: evidence for the inhibition of angiotensin converting enzyme. J. Ethnopharmacol., **134**, 363-372.
Ghowsi, M., Khazali, H. and Sisakhtnezhad, S. (2018): Evaluation of *TNF-α* and *IL-6* mRNAs expressions in visceral and subcutaneous adipose tissues of polycystic ovarian rats and effects of resveratrol. Iran. J. Basic Med. Sci., **21**, 165-174.
Gong, C., Wang, T.W., Huang, H.S. and Parent, J.M. (2007): Reelin regulates neuronal progenitor migration in intact and epileptic hippocampus. J. Neurosci., **27**, 1803-1811.
Gulyás, A.I., Hájos, N. and Freund, T.F. (1996): Interneurons containing calretinin are specialized to control other interneurons in the rat hippocampus. J. Neurosci., **16**, 3397-3411.
Guzowski, J.F. (2002): Insights into immediate-early gene function in hippocampal memory consolidation using antisense oligonucleotide and fluorescent imaging approaches. Hippocampus, **12**, 86-104.
Guzowski, J.F., Timlin, J.A., Roysam, B., McNaughton, B.L., Worley, P.F. and Barnes, C.A. (2005): Mapping behaviorally relevant neural circuits with immediate-early gene expression. Curr. Opin. Neurobiol., **15**, 599-606.
Hanson, N.D., Owens, M.J. and Nemeroff, C.B. (2011): Depression, antidepressants, and neurogenesis: a critical reappraisal. Neuropsychopharmacology, **36**, 2589-2602.
Haroz, E.E., Ritchey, M., Bass, J.K., Kohrt, B.A., Augustinavicius, J., Michalopoulos, L., Burkey, M.D. and Bolton, P. (2017): How is depression experienced around the world? A systematic review of qualitative literature. Soc. Sci. Med., **183**, 151-162.
Hodge, R.D., Kowalczyk, T.D., Wolf, S.A., Encinas, J.M., Rippey, C., Enikolopov, G., Kempermann, G. and Hevner, R.F. (2008): Intermediate progenitors in adult hippocampal neurogenesis: Tbr2 expression and coordinate regulation of neuronal output. J. Neurosci., **28**, 3707-3717.
Huang, X., Hussain, B. and Chang, J. (2021): Peripheral inflammation and blood-brain barrier disruption: effects and mechanisms. CNS Neurosci. Ther., **27**, 36-47.
Jamali-Raeufy, N., Alizadeh, F., Mehrabi, Z., Mehrabi, S. and Goudarzi, M. (2021): Acetyl-L-carnitine confers neuroprotection against lipopolysaccharide (LPS) -induced neuroinflammation by targeting TLR4/NFκB, autophagy, inflammation and oxidative stress. Metab. Brain Dis., **36**, 1391-1401.
Jurga, A.M., Paleczna, M. and Kuter, K.Z. (2020): Overview of General and Discriminating Markers of Differential Microglia Phenotypes. Front. Cell. Neurosci., **14**, 198.
Kangawa, Y., Yoshida, T., Abe, H., Seto, Y., Miyashita, T., Nakamura, M., Kihara, T., Hayashi, S.M. and Shibutani, M. (2017): Anti-inflammatory effects of the selective phosphodiesterase 3 inhibitor, cilostazol, and antioxidants, enzymatically-modified isoquercitrin and α-lipoic acid, reduce dextran sulphate sodium-induced colorectal mucosal injury in mice. Exp. Toxicol. Pathol., **69**, 179-186.
Kempermann, G., Song, H. and Gage, F.H. (2015): Neurogenesis in the Adult Hippocampus. Cold Spring Harb. Perspect. Biol., **7**, a018812.
Li, J., Serafin, E. and Baccei, M.L. (2018): Prostaglandin Signaling Governs Spike Timing-Dependent Plasticity at Sensory Synapses onto Mouse Spinal Projection Neurons. J. Neurosci., **38**, 6628-6639.
Liddelow, S.A., Guttenplan, K.A., Clarke, L.E., Bennett, F.C., Bohlen, C.J., Schirmer, L., Bennett, M.L., Münch, A.E., Chung, W.S., Peterson, T.C., Wilton, D.K., Frouin, A., Napier, B.A., Panicker, N., Kumar, M., Buckwalter, M.S., Rowitch, D.H., Dawson, V.L., Dawson, T.M., Stevens, B. and Barres, B.A. (2017): Neurotoxic reactive astrocytes are induced by activated microglia. Nature, **541**, 481-487.
Liu, L.R., Liu, J.C., Bao, J.S., Bai, Q.Q. and Wang, G.Q. (2020): Interaction of Microglia and Astrocytes in the Neurovascular Unit. Front. Immunol., **11**, 1024.
Livak, K.J. and Schmittgen, T.D. (2001): Analysis of relative gene expression data using real-time quantitative PCR and the $2^{-\Delta\Delta C_T}$ Method. Methods, **25**, 402-408.
Makino, T., Kanemaru, M., Okuyama, S., Shimizu, R., Tanaka, H. and Mizukami, H. (2013): Anti-allergic effects of enzymatically modified isoquercitrin (α-oligoglucosyl quercetin 3-O-glucoside), quercetin 3-O-glucoside, α-oligoglucosyl rutin, and quercetin, when administered orally to mice. J. Nat. Med., **67**, 881-886.
Masubuchi, Y., Nakahara, J., Kikuchi, S., Okano, H., Takahashi, Y., Takashima, K., Koyanagi, M., Maronpot, R.R., Yoshida, T., Hayashi, S.M. and Shibutani, M. (2020): Continuous exposure to α-glycosyl isoquercitrin from developmental stages to adulthood is necessary for facilitating fear extinction learning in rats. J. Toxicol. Pathol., **33**, 247-263.
Miller, S.M. and Sahay, A. (2019): Functions of adult-born neurons in hippocampal memory interference and indexing. Nat. Neurosci., **22**, 1565-1575.
Minatohara, K., Akiyoshi, M. and Okuno, H. (2016): Role of Immediate-Early Genes in Synaptic Plasticity and Neuronal Ensembles Underlying the Memory Trace. Front. Mol. Neurosci., **8**, 78.
Moreno-Jiménez, E.P., Terreros-Roncal, J., Flor-García, M., Rábano, A. and Llorens-Martín, M. (2021): Evidences for Adult Hippocampal Neurogenesis in Humans. J. Neurosci., **41**, 2541-2553.
Okada, R., Masubuchi, Y., Tanaka, T., Nakajima, K., Masuda, S., Nakamura, K., Maronpot, R.R., Yoshida, T., Koyanagi, M., Hayashi, S.M. and Shibutani, M. (2019): Continuous exposure to α-glycosyl isoquercitrin from developmental stage facilitates fear extinction learning in rats. J. Funct. Foods, **55**, 312-324.
Ponnappan, U. (1998): Regulation of transcription factor NF kappa B in immune senescence. Front. Biosci., **3**, d152-d168.

Pujadas, L., Gruart, A., Bosch, C., Delgado, L., Teixeira, C.M., Rossi, D., de Lecea, L., Martínez, A., Delgado-García, J.M. and Soriano, E. (2010): Reelin regulates postnatal neurogenesis and enhances spine hypertrophy and long-term potentiation. J. Neurosci., **30**, 4636-4649.

Salmani, H., Hosseini, M., Beheshti, F., Baghcheghi, Y., Sadeghnia, H.R., Soukhtanloo, M., Shafei, M.N. and Khazaei, M. (2018): Angiotensin receptor blocker, losartan ameliorates neuroinflammation and behavioral consequences of lipopolysaccharide injection. Life Sci., **203**, 161-170.

Sibbe, M. and Kulik, A. (2017): GABAergic Regulation of Adult Hippocampal Neurogenesis. Mol. Neurobiol., **54**, 5497-5510.

Song, C. and Wang, H. (2011): Cytokines mediated inflammation and decreased neurogenesis in animal models of depression. Prog. Neuropsychopharmacol. Biol. Psychiatry, **35**, 760-768.

Spanos, F. and Liddelow, S.A. (2020): An Overview of Astrocyte Responses in Genetically Induced Alzheimer's Disease Mouse Models. Cells, **9**, 2415.

Tanaka, T., Masubuchi, Y., Okada, R., Nakajima, K., Nakamura, K., Masuda, S., Nakahara, J., Maronpot, R.R., Yoshida, T., Koyanagi, M., Hayashi, S.M. and Shibutani, M. (2019): Ameliorating effect of postweaning exposure to antioxidant on disruption of hippocampal neurogenesis induced by developmental hypothyroidism in rats. J. Toxicol. Sci., **44**, 357-372.

Taniguti, E.H., Ferreira, Y.S., Stupp, I.J., Fraga-Junior, E.B., Doneda, D.L., Lopes, L., Rios-Santos, F., Lima, E., Buss, Z.S., Viola, G.G. and Vandresen-Filho, S. (2019): Atorvastatin prevents lipopolysaccharide-induced depressive-like behaviour in mice. Brain Res. Bull., **146**, 279-286.

von Bohlen Und Halbach, O. (2007): Immunohistological markers for staging neurogenesis in adult hippocampus. Cell Tissue Res., **329**, 409-420.

Walker, D.G. and Lue, L.F. (2015): Immune phenotypes of microglia in human neurodegenerative disease: challenges to detecting microglial polarization in human brains. Alzheimers Res. Ther., **7**, 56.

Wang, X., Zhu, L., Hu, J., Guo, R., Ye, S., Liu, F., Wang, D., Zhao, Y., Hu, A., Wang, X., Guo, K. and Lin, L. (2020): FGF21 Attenuated LPS-Induced Depressive-Like Behavior *via* Inhibiting the Inflammatory Pathway. Front. Pharmacol., **11**, 154.

Zhang, B., Wang, P.P., Hu, K.L., Li, L.N., Yu, X., Lu, Y. and Chang, H.S. (2019): Antidepressant-Like Effect and Mechanism of Action of Honokiol on the Mouse Lipopolysaccharide (LPS) Depression Model. Molecules, **24**, 2035.